Effect of Elasticity Parameter on Viscoelastic Fluid in Pipe Flow Using Extended Pom-Pom Model

Khorsand Movagar, Mohammad Reza; Rashidi, Fariborz*[+]

Faculty of Chemical Engineering, Amirkabir University of Technology, Tehran, I.R. IRAN

Goharpey, Fatemeh

Faculty of Polymer Engineering, Amirkabir University of Technology, Tehran, I.R. IRAN

Mirzazadeh, Mahmoud

Faculty of Chemical Engineering, Amirkabir University of Technology, Tehran, I.R. IRAN

Amani, Ehsan

Faculty of Mechanical Engineering, Amirkabir University of Technology, Tehran, I.R. IRAN

ABSTRACT: *In this study prediction of the steady-state flow of branched polymer melts in pipe geometry with finite volume method is presented. Our analysis in this study revealed that; for normal-stress $\tau_{\theta\theta}$, the XPP model can predict this tensor unlike the other viscoelastic models such as PTT or Gieskus which can not predict $\tau_{\theta\theta}$ for viscoelastic fluid in two dimensional pipe flows. The fluid is modelled using a modification of the Pom-Pom model known as the single eXtended Pom-Pom (XPP) where viscoelastic fluid is typically a commercial low-density polyethylene. In finite volume method, the operator-integration is used to discretize the governing equations in space or control volume. An iterative solution algorithm that decouples the computation of momentum from that of stress is used to solve the discrete equations. Numerical results are presented, including the profiles of all relevant stresses, the axial velocity, stretch and the viscosity across the gap, demonstrating the performance of the model predictions. The influence of elasticity parameter on flow behaviour is studied, which demonstrates in particular, the dependence of velocity and stresses distribution as a function of Weissenberg number is analyzed. Also, the effect of Weissenberg number on pressure gradient has been considered. Finally, verification of the present model was made by comparing to the Generalized Newtonian Fluid (GNF) model.*

KEY WORDS: *Viscoelastic flow, Extended Pom-Pom, Finite volume method, Pipe flow.*

INTRODUCTION

Polymer melts with long-chain side branches have rheological properties that differ distinctly from those of linear polymers that have side branches too short to entangle with surrounding polymers. The idealized molecule,

* *To whom correspondence should be addressed.*
+ *E-mail: rashidi@aut.ac.ir*
1021-9986/10/3/85 12/$/3.20

such as Low Density Polyethylene (LDPE), is called a "pom-pom" molecule, which has multiple branch points per molecule. Because these branches are entangled with surrounding molecule, the backbone can readily be stretched in an extensional flow, and show a strain-hardening, while in shearing flows, the behaviour is highly strain-softening, much like that of un- branched polymers. Hence branched polymers have flow properties that are strongly dependent on the molecular topology; wheras ordinary linear polymers typically show predominantly strain-softening characteristics in both shear and extensional flows.

In the investigation of the rheology of polymer melts, the main problem is to get a correct nonlinear behaviour in both shear and extension. Most of the traditional constitutive models such as PTT, Gieskus and K-BKZ are unable to overcome this difficulty.

Mc Liesh & Larson [1] have introduced a new constitutive model for branched polymers, known as pom-pom model, that overcomes this shortcoming. This model is based on tube theory [2] and a simplified form of branched molecules. The model consists of two decoupled equations, one for orientation another for stretch; separation of relaxation times for this stretch and orientation is key feature for this model [3]. There have made modifications to the original pom-pom model [4]. They consist of multiple modes that show quantitative agreement between experiments and model predictions by using numerical simulation techniques [5]. Also these multiple modes permit the fitting of Low-Density Polyethylene (LDPE) rheology data [6].

The original pom–pom model suffers from three problems. First, the model predicts a zero second normal stress difference. Secondly, there is an unphysical discontinuity in the gradient of the extensional viscosity when the stretch is equal to q at steady state. Thirdly, the shear stress has a maximum. *Verbeeten et al.* [3] introduced a modified model, the eXtended Pom-Pom (XPP) model, to circumvent these three problems.

A modification made to the stretch equation, by *Blackwell et al.* [7], which allows for branch point displacement to overcome the discontinuity in the gradient of the extensional viscosity. The retraction of the arms into the tube has been neglected, and thereby the constraint that the stretch cannot be larger than the number of arms is removed. A Giesekus-like term has been added to the orientation equation, to introduce a non-zero second normal stress difference. Furthermore, the orientation equation is bounded for high strain rates. The XPP model was successfully implemented in a finite element method and good quantitative agreement was found in comparisons between experiments with LDPE melts and numerical simulations using a multi-mode XPP model [5,6,8,9].

In the last decade, there have been many numerical studies regarding XPP model; most of them considering contraction planar geometry. Finite element methods (spectral element methods) were employed by *Verbeeten et al.* [9], *Phillips & van Os* [5] basically on the prediction of elongation flow on contraction planar and flow past a cylinder geometry. On the other hand, some finite volume methods [10,11] or hybrid method [12] which contain FV/FE together have been applied to numerical predictions of viscoelastic fluid on contraction planar flow and poiseuille flow in a planar channel.

The main objective of present work was the study of the velocity and stresses profile in Poiseuille pipe flow at different Weissenberg numbers. In this study a numerical study to investigate the use of finite volume method in predicting the steady-state flow of viscoelastic fluid in a pipe, was accomplished and single-equation XPP model was used to realistically describe the rheology behaviour in pipe geometry.

THEORETICAL SECTION

Governing equations

The governing equations comprise the conservation equations of momentum and mass, together with a rheological equation of state. In this paper the Single equation version of the eXtended Pom-Pom (SXPP) model is considered. The equations of motion and continuity are

$$\nabla.u = 0 \tag{1}$$

$$\rho\left(\frac{\partial u}{\partial t} + u.\nabla u\right) = -\nabla p + \nabla.\tau + \eta_s \nabla^2 u \tag{2}$$

where u is the velocity field, ρ is the density, η_s is the solvent viscosity, p is the pressure and τ is the polymeric contribution to the extra-stress tensor. The constitutive equation for the single equation version of the XPP model is

$$f(\lambda, \tau)\tau + \lambda_{0b}\overset{\nabla}{\tau} + G_0(f(\lambda, \tau) - 1)I + \frac{\alpha}{G_o}\tau \cdot \tau = 2\lambda_{0b}G_0 d \tag{3}$$

where

$$f(\lambda,\tau) = 2\frac{\lambda_{ob}}{\lambda os} e^{\nu(\lambda-1)}(1-\frac{1}{\lambda}) + \frac{1}{\lambda^2}[1-\frac{\alpha I_{\tau.\tau}}{3G_0^2}] \quad (4)$$

In these equations λ_{0b} and λ_{0s} are the orientation and backbone stretch relaxation times, respectively, and G_0 is the linear relaxation modulus. The constitutive equation possesses features of the Giesekus model since a non-zero second normal stress difference is predicted when $\alpha \neq 0$. In the SXPP model, the backbone stretch is directly coupled to the extra stress tensor

$$\lambda = \sqrt{1+\frac{I_\tau}{3G_o}} \quad (5)$$

The parameter ν in Eq. (4) was incorporated into the model to remove the discontinuity in the derivative of the extensional viscosity that was present in the differential approximation of the original pom-pom model. Its value is estimated by data fitting and found to be inversely proportional to the number of arms (q). More precisely, we have

$$\nu = \frac{2}{q} \quad (6)$$

Finally, the extra-stress tensor can be written as the sum of polymeric and solvent contributions, i.e.

$$T = \tau + 2\eta_s d \quad (7)$$

The governing equations are non-dimensionalised via length scale L, velocity scale U, time scale L/U, and pressure and extra-stress scales of ηU/L, where L is unit length, U is the mean velocity (taking a unit flow rate for Pipe radius), and $\eta = \eta_s + \eta_p$ is the total viscosity. To preserve a similarity between the form of the non-dimensional Oldroyd-B and SXPP models, we define $\mu_p = G_0\lambda_{0b}$. Then, defining dimensionless parameters, the Reynolds number (Re), the Weissenberg number or elasticity parameter (We), the viscosity ratio parameter (β) and the ratio of two relaxation times parameter (ε) are as follow:

$$Re = \frac{\rho UL}{\eta},\ We = \frac{\lambda_{ob}U}{L},\ \beta = \frac{\eta_s}{\eta_s + G_0\lambda_{0b}},\ \varepsilon = \frac{\lambda_{0s}}{\lambda_{0b}} \quad (8)$$

The governing equations may be written in the non-dimensional form

$$\nabla \cdot u = 0 \quad (9)$$

$$Re\left(\frac{\partial u}{\partial t} + u.\nabla u\right) = -\nabla p + \nabla.\tau + \beta\nabla^2 u \quad (10)$$

while the non-dimensional single equation XPP model Eqs. (11)-(13) is given by [6]:

$$f(\lambda,\tau)\tau + We\overset{\nabla}{\tau} + \frac{1-\beta}{We}(f(\lambda,\tau)-1)I + \frac{\alpha We}{1-\beta}\tau\cdot\tau = 2(1-\beta)d \quad (11)$$

where f (λ,τ) and λ, are given by:

$$f(\lambda,\tau) = \frac{2}{\varepsilon}(1-\frac{1}{\lambda})e^{\nu(\lambda-1)} + \frac{1}{\lambda^2}[1-(\frac{We}{1-\beta})^2\frac{\alpha}{3}I_{\tau.\tau}] \quad (12)$$

and

$$\lambda = \sqrt{1+\frac{We}{(1-\beta)}\frac{1}{3}I_\tau} \quad (13)$$

The parameter ε, the ratio of the stretch to orientation relaxation times, is inversely proportional to the entanglement molecular weight of the backbone segments. So that values of ε approaching unity correspond to molecules with relatively short backbone lengths but long arms to slow down the dynamics, and small values of ε correspond to highly entangled backbones.

Note, that the Oldroyd-B model corresponds to setting α = 0 and f (λ, τ) = 1 in Eq. (11). If, in addition, β = 0 then the UCM model is obtained.

Finite volume scheme

Finite volume discretisation

The finite volume method is generally applied to a system of equations written in conservative form.

Here, we consider cell-centred finite volume methods for discretising the governing equations. The common form of conservation laws for each of the governing Eqs. (9)–(11), in 2D axisymmetric flow, is as follow:

$$\delta\frac{\partial\phi}{\partial t} + \frac{\partial}{\partial Z}\left(u\phi\theta - \Gamma\frac{\partial\phi}{\partial Z}\right) + \frac{1}{r}\frac{\partial}{\partial r}\left(rV\phi\theta - r\Gamma\frac{\partial\phi}{\partial r}\right) = S_\phi \quad (14)$$

for cylindrical coordinates, where δ, θ, and Γ are constants, and φ and Sφ are functions that are defined depending on the particular equation under consideration (Table1).

Table 1: Definition of constants and functions in the general equation.

Equation	ϕ	δ	θ	Γ	$S\phi$
u-momentum	u	Re	Re	β	$-\frac{\partial p}{\partial Z}+\frac{\partial \tau_{zz}}{\partial Z}+\frac{1}{r}\frac{\partial}{\partial r}\left(r\tau_{rz}\right)$
V-momentum	V	Re	Re	β	$-\frac{\partial p}{\partial r}+\frac{u}{r^2}+\frac{1}{r}\frac{\partial}{\partial r}\left(r\tau_{rr}\right)+\frac{\partial \tau_{rz}}{\partial Z}-\frac{\tau_{\theta\theta}}{r}$
τ_{zz} Normal stress	τ_{zz}	We	We	0	$2(1-\beta)\frac{\partial u}{\partial Z}+2We\tau_{zz}\frac{\partial u}{\partial Z}+2We\tau_{rz}\frac{\partial u}{\partial r}-f(\lambda,\tau)\tau_{zz}-\{f(\lambda,\tau)-1\}\frac{1-\beta}{We}-\alpha\frac{We}{1-\beta}\left(\tau_{zz}^2+\tau_{rz}^2\right)$
τ_{rr} Normal stress	τ_{rr}	We	We	0	$2(1-\beta)\frac{\partial V}{\partial r}+2We\tau_{rr}\frac{\partial V}{\partial r}+2We\tau_{rz}\frac{\partial V}{\partial Z}-f(\lambda,\tau)\tau_{rr}-\{f(\lambda,\tau)-1\}\frac{1-\beta}{We}-\alpha\frac{We}{1-\beta}\left(\tau_{rr}^2+\tau_{rz}^2\right)$
$\tau_{\theta\theta}$ Normal stress	$\tau_{\theta\theta}$	We	We	0	$2(1-\beta)\frac{V}{r}+2We\tau_{\theta\theta}\frac{V}{r}-f(\lambda,\tau)\tau_{\theta\theta}-\{f(\lambda,\tau)-1\}\frac{1-\beta}{We}-\alpha\frac{We}{1-\beta}\left(\tau_{\theta\theta}^2\right)$
τ_{rz} Normal stress	τ_{rz}	We	We	0	$(1-\beta)\left(\frac{\partial V}{\partial Z}+\frac{\partial u}{\partial r}\right)+We\tau_{rz}\left(\frac{\partial u}{\partial Z}+\frac{\partial V}{\partial r}\right)+We\tau_{zz}\frac{\partial V}{\partial Z}+We\tau_{rr}\frac{\partial u}{\partial r}-f(\lambda,\tau)\tau_{rz}-\alpha\frac{We}{1-\beta}\tau_{rz}\left(\tau_{rr}+\tau_{zz}\right)$
Continuity	1	0	1	0	0

The computational grid

A reference grid is considered for computational domain and a control volume is associated with each unknown on the grid. The sides of each control volume are aligned with the coordinate axes. Each component of Eq. (14) is integrated over an appropriate control volume. In the finite volume formulation, mass and momentum are conserved over every control volume and therefore over the whole computational domain.

The property of conservation of physical quantities, which is preserved by the discrete system, is one of the attractions of the finite volume method. In this paper, a staggered grid is used in which the dependent variables are located at different points as shown in Fig. 1 for the axisymmetric. This figure shows that the normal and shear stresses are located at the corners of mesh cells. This configuration of staggered grid has some advantages, at first it reduces the need for interpolations of stress components values in the momentum equations and secondly, the satisfying of boundary conditions is performed better.

This mesh ensures that the solution is not polluted by the spurious pressure modes which may be present on collocated meshes.

Discretization

The generalized time discretised algebraic equations for continuity, momentum are as follows:

$$\nabla . u^{n+1} = 0 \tag{15}$$

$$Re\left(\frac{u^{n+1}-u^{*n}}{\Delta t}+u^{n+1}\cdot\nabla u^{n+1}\right)-\beta\nabla^2 u^{n+1}+ \tag{16}$$

$$\nabla P^{n+1} = \nabla\cdot\tau^{n}$$

In discretising the convection – diffusion terms of the momentum equations, power-law scheme which is the modified version of hybrid scheme, has been employed. In the conventional hybrid scheme, when the cell Peclet number is larger than some reference value, upwind difference is taken for convection terms, whereas when it is smaller, central difference is taken for them. The treatment of the convection-diffusion terms in momentum equations using finite volume method was described by *Patankar* (1983) [13]. Integrating the momentum equations over the control volume shown in Fig. 2, approximates derivatives using finite differences, which leads to the final two-dimensional discretisation equation that can be written as follow:

$a_p \Phi_P = a_E \Phi_E + a_W \Phi_W + a_N \Phi_N + a_S \Phi_S + b$

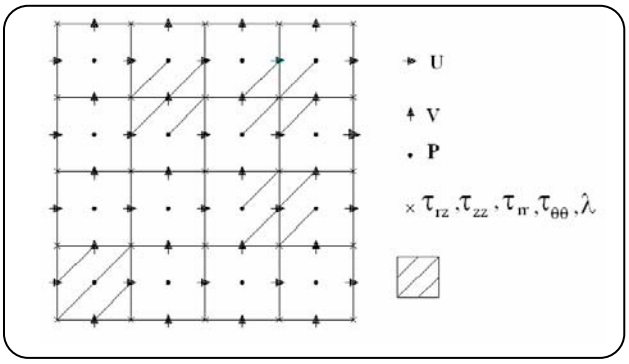

Fig. 1: Location of the variables on the finite volume grids.

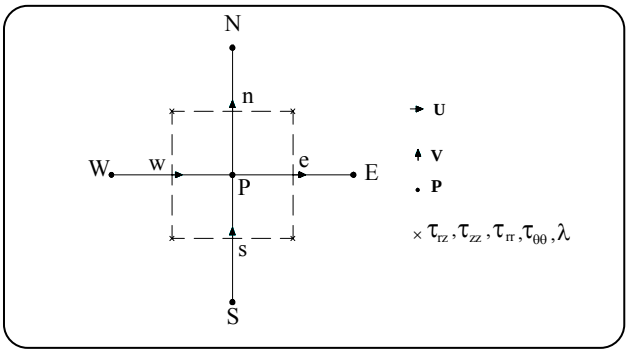

Fig. 2: A general control volume.

where a_i coefficients are function of Peclet number as $A|Pe|$. In order to power-law discretisation, $A|Pe|$ is defined as follow:

$$A|Pe| = \left\| 0, \left(1 - 0.1|Pe|\right)^5 \right\| \quad \text{(Pe, is Peclet number)}$$

The operator $\|A, B\|$ denotes the grater of A and B. The reader is referred to *Patankar* [13] for further details.

The generalized time discretised algebraic equation for stress is as follows:

$$We\left(\frac{\tau^{n+1} - \tau^{*n}}{\Delta t}\right) + \tag{17}$$

$$We\left(u^n \cdot \nabla T^{n+1} - \left(\nabla u^T\right)^n \cdot T^{n+1} + T^{n+1} \cdot \left(\nabla u\right)^n\right) +$$

$$f\left(\lambda^n, \tau^n\right)\tau^{n+1} + \alpha\frac{We}{1-\beta}\tau^{n+1} \cdot \tau^{n+1} =$$

$$2(1-\beta)d^n - \left\{f\left(\lambda^n, \tau^n\right) - 1\right\}\frac{1-\beta}{We}I$$

For stress components equations including shear stress τ_{rz} and normal stresses τ_{zz}, τ_{rr}, $\tau_{\theta\theta}$ equations, the diffusion term is zero, therefore for treatment of convection term the upwind difference is considered.

The most complex part of equations, which are listed in Table 1, is integrating of the source term S_ϕ over the general control volume shown in Fig. 2. The typicall result obtained for normal stress τ_{zz}, using finite difference approximation for the velocity derivatives, is as follow:

$$We\left(\frac{\left(\tau_{zz}^{n+1}\right)_p - \left(\tau_{zz}^{*n}\right)_p}{\Delta t}\right) r_p \Delta r \Delta z = \tag{18}$$

$$2(1-\beta)\left(u_e - u_w\right) r_p \Delta r + 2We\left(u_e - u_w\right)\left(\tau_{zz}^{n+1}\right)_p r_p \Delta r +$$

$$2We\left(u_n - u_s\right)\left(\tau_{rz}^{n+1}\right)_p r_p \Delta z -$$

$$r_p \Delta r \Delta z \left\{ \begin{array}{l} f\left(\lambda^n, \tau^n\right)\left(\tau_{zz}^{n+1}\right)_p + \left(f\left(\lambda^n, \tau^n\right) - 1\right)\frac{1-\beta}{We} I + \\ \alpha\frac{We}{1-\beta}\left[\left(\tau_{zz}^{n+1}\right)_P^2 + \left(\tau_{rz}^{n+1}\right)_P^2\right] \end{array} \right\}$$

where Δr and Δz are the radial and axial lengths of the control volume. Table 2 gives the expressions for the integrated source term for each of the component equations.

There is no difficulty in evaluating most of the terms as the variables are defined at the points on the grid where we need to approximate them. However, the last terms in the τ_{zz} and τ_{rr} source terms, the terms involving the $u_{r\,(P)}$ variable in the $\tau_{\theta\theta}$ source term, and the terms involving the normal stress variables in the shear stress source term are undefined at the points where they are required. These terms are approximated by taking an average of the relevant variables at the points which immediately surround the unknown, and using finite difference approximations for the velocity derivatives.

Solution algorithm

The generalized time at staggered axisymmetric grid is employed for discretising the governing equations based on the SIMPLER algorithm [13]. For the solution of the set of non-linear algebraic equations (coupled system), the Three Diagonal Matrix Algorithm (TDMA) method is used by employing a line by line scheme. This procedure is followed for all the lines in one direction and is repeated, if necessary, for the other lines in the other direction. In the iteration of linearized equations for u, v, p, τ_{zz}, τ_{rr}, $\tau_{\theta\theta}$ and τ_{rz}, under relaxation parameter are used and appropriate artificial viscosity terms are included.

The skeleton of the algorithm is described here. Each time step comprises the following key stages:

Table 2: The component expression for the source terms after numerical integration.

Φ	$\int_{w}^{e}\int_{s}^{n} S_{\Phi}\, r\, dr\, dz$
u	$\left(P_w - P_e\right) r_p \Delta r + \left[r_n \tau_{rz(n)} - r_s \tau_{rz(s)} \right] \Delta Z + \left[\tau_{zz(e)} - \tau_{zz(w)} \right] r_p \Delta r$
V	$\left(P_s - P_n\right) r_p \Delta Z - \frac{V_p}{r_p} \Delta r \Delta Z + \left[\tau_{rz(e)} - \tau_{rz(w)} \right] \Delta Z + \left(\tau_{zz(e)} - \tau_{zz(w)} \right) r_p \Delta r + \left[r_n \tau_{rr(n)} - r_s \tau_{rr(s)} \right] \Delta Z - \tau_{\theta\theta} \Delta r \Delta Z$
τ_{zz}	$-\frac{\alpha We}{1-\beta} r_p \Delta r \Delta Z \tau_{zz(p)}^2 + \left[2We r_p \Delta r \left(u_e - u_w \right) - f_p r_p \Delta r \Delta Z \right] \tau_{zz(p)} + \left[2\left(1-\beta\right) r_p \Delta r \left(u_e - u_w \right) + 2We \tau_{rz(p)} r_p \Delta Z \left(u_n - u_s \right) - \left(\frac{\alpha We}{1-\beta} \tau_{rz(p)}^2 + \left(f_p - 1 \right) \frac{1-\beta}{We} \right) r_p \Delta r \Delta Z \right]$
τ_{rr}	$-\frac{\alpha We}{1-\beta} r_p \Delta r \Delta Z \tau_{rr(p)}^2 + \left[2We r_p \Delta Z \left(V_n - V_s \right) - f_p r_p \Delta r \Delta Z \right] \tau_{rr(p)} + \left[2\left(1-\beta\right) r_p \Delta Z \left(V_n - V_s \right) + 2We \tau_{rz(p)} r_p \Delta r \left(V_e - V_w \right) - \left(\frac{\alpha We}{1-\beta} \tau_{rz(p)}^2 + \left(f_p - 1 \right) \frac{1-\beta}{We} \right) r_p \Delta r \Delta Z \right]$
$\tau_{\theta\theta}$	$-\frac{\alpha We}{1-\beta} r_p \Delta r \Delta Z \tau_{\theta\theta(p)}^2 + \left[2We \frac{V_p}{r_p} - f_p \right] r_p \Delta r \Delta Z \tau_{\theta\theta(p)} + \left[2\left(1-\beta\right) \frac{V_p}{r_p} - \left(f_p - 1 \right) \frac{1-\beta}{We} \right] r_p \Delta r \Delta Z$
τ_{rz}	$-\left[We \frac{V_p}{r_p} + f_p + \frac{\alpha We}{1-\beta} \left(\tau_{rr(p)} + \tau_{zz(p)} \right) \right] r_p \Delta r \Delta Z + \left[\left(1-\beta\right) + We \tau_{zz(p)} \right] \left(V_e - V_w \right) r_p \Delta r + \left[\left(1-\beta\right) + We \tau_{rr(p)} \right] \left(u_n - u_s \right) r_p \Delta Z$

• Semi-Lagrangian stage: The values of u^{*n} and T^{*n} are calculated by determining the departure points of the relevant control volumes and performing area-weighting.

• SIMPLER stage: The conservation Eqs. (15) & (16) are solved using a pressure correction equation to ensure that the velocity field u^{*n+1} is divergence-free.

• Viscoelastic stage: The system of algebraic Eq. (17) is solved to determine T^{*n+1}.

The flowchart of the algorithm is presented in appendix.

This process is repeated until a steady-state solution is obtained. The extension of this algorithm to viscoelastic problems has been described in detail in *Phillips & Williams* [10].

Poiseuille Flow in a pipe

Because of complexity of the stress equations, the solution of steady-state flow problems with XPP model differs from other viscoelastic models. For model fluids of Maxwell/Oldroyd type, the governing equations possess an analytical solution for the transient development of the velocity and extra-stress profiles for plane Poiseuille flow [14]. However, the governing equations for the extended pom-pom class of models do not possess an equivalent analytical steady-state solution. Therefore, the fully-developed steady-state solution of the problem needs to be determined numerically.

In this study, we determine the steady-state solution for an XPP fluid and describe the effect of the model parameters on velocity profile, stretch and components of the polymeric contribution to the extra-stress tensor. Parameter continuation in Weissenberg number is used to obtain numerical solutions at high values of the Weissenberg number. To obtain the steady-state solution for the XPP model for a given flow rate, boundary conditions are supposed as follow:

-Inlet: The inflow conditions are chosen to be those corresponding to the Oldroyd-B model with the same flow rate. Inflow conditions are specified for velocity and stress components.

-Wall: No-slip boundary conditions are imposed on the pipe walls

-Symmetry: Axisymmetry is imposed at the centreline from inlet to outlet of the pipe, So the fluid has a maximum axial velocity and zero radial velocity, and at the axis of symmetry leading stress components are set to be zero at the center line.

-Outlet: We assume that the pipe length is long enough to satisfy fully developed flow at the out flow. So the inflow profiles develop through the pipe and attain desired XPP profiles at outflow.

A rectangular coordinate geometry which contains non-uniformed structured 30 × 60 mesh with a computational domain of [0,2] × [0,20] is employed for finite volume scheme. Computations were also performed on a structured 60 × 100 mesh to ensure that convergence of the approximations with mesh refinement was achieved.

In our study we assume *R,* for a radius of pipe, r, for the radial-stream coordinate and v, for the radial velocity. In this geometry, z is the streamwise coordinate and u is axial velocity. The coordinate system used is centre (r = 0) on the axisymmetry or centerline and (r = R) at the wall.

RESULTS AND DISCUSSION

Effect of We

Fig. 3 shows the effect of the Weissenberg number or elasticity parameter on the profiles of stretch, velocity, and polymeric contributions to the extra stress components τ_{zz}, τ_{rr}, $\tau_{\theta\theta}$ and τ_{rz} For this purpose, the other model parameters are constant and are taken to be Re = 1, q = 2, $\varepsilon = 1/3$, $\beta = 1/9$ and $\alpha = 0.15$.

At constant flow rate (unit flow rate) and corresponding pressure gradient, as Weissenberg number increases, the velocity profiles flatten in the center which indicates stronger shear-thinning behavior. The Pom-Pom model demonstrates a more severe form of shear-thinning in which there is a range of shear rates, where the shear stress decreases with the increase in flow rate (see [15]). The maximum value of the velocity at We = 1 is 1.85 that exhibits smaller maximum value than for the Newtonian or UCM fluid (2.0) when the same flow rate is considered. These values decrease to 1.67 and 1.63, respectively, when We = 3 and We = 7. The influence of mesh refinement for this scheme is to change the approximations to the maximum value of velocity by less than 0.1%.

The stretch takes its equilibrium value in the centre of the pipe. Its maximum value, occurring on the wall, increases as Weissenberg number increases. The stretch, in all cases, has its equilibrium value ($\lambda = 1$) in the middle of the pipe. When the size of velocity gradient is greater, the larger value of stretch is obtained.

For the shear-stress τ_{rz} tensor, we observe its decrease when the Weissenberg number increases and a linear contribution for the Newtonian stress was observed, only for the region that λ is near its equilibrium value; for We = 1, this extra-stress component profile is nearly linear.

On the other hand, for normal-stresses τ_{zz}, τ_{rr} tensors, we observe that they grow when the Weissenberg number increases but τ_{rr} tensor relaxes at higher value of *We***.**

Note that, for normal-stress $\tau_{\theta\theta}$, the XPP model can predict this tensor unlike the other viscoelastic models such as PTT or Gieskus which can not predict $\tau_{\theta\theta}$ for viscoelastic fluid in two dimensional pipe flows. As it can be seen when the Weissenberg number increases, $\tau_{\theta\theta}$ increases similar to the behaviour of the two other normal-stresses.

It is clear from velocity profile in figure 3 that for identical pressure gradients, the XPP fluid can carry a larger flow rate than the Newtonian or UCM fluids. This effect is due to an increased shear-thinning behavior with the Weissenberg number (Fig.4).

Pressure gradient study

In engineering calculations involving polymer flows in ducts, in determining pressure drop and pumping capacity we need an expression for fRe, where f is the Fanning friction factor usually defined as:

$$f = \nabla p \frac{R}{\rho U^2} \tag{19}$$

where ∇P is non-dimensional pressure drop, R half-width radius, ρ density of fluid and U is average velocity.

Using the definition of Reynolds number (Eq. (8)) and after some algebra arrangement, we arrive at the following expression for f Re:

$$f\,Re = 16\nabla p \tag{20}$$

In Fig.5, we make predictions for pressure gradient ∇P, equivalent to non-dimensional pressure drop/pipe length, as a function of Weissenberg number with Re = 1, q = 2, $\varepsilon = 1/3$, $\beta = 1/9$ and $\alpha = 0.15$. This figure shows that pressure gradient descends with ascending Weissenberg number for the range considered.

Verification with generalized Newtonian fluid (GNF) modle

In this section, the results obtained from the XPP model will be compared with those of a Generalized

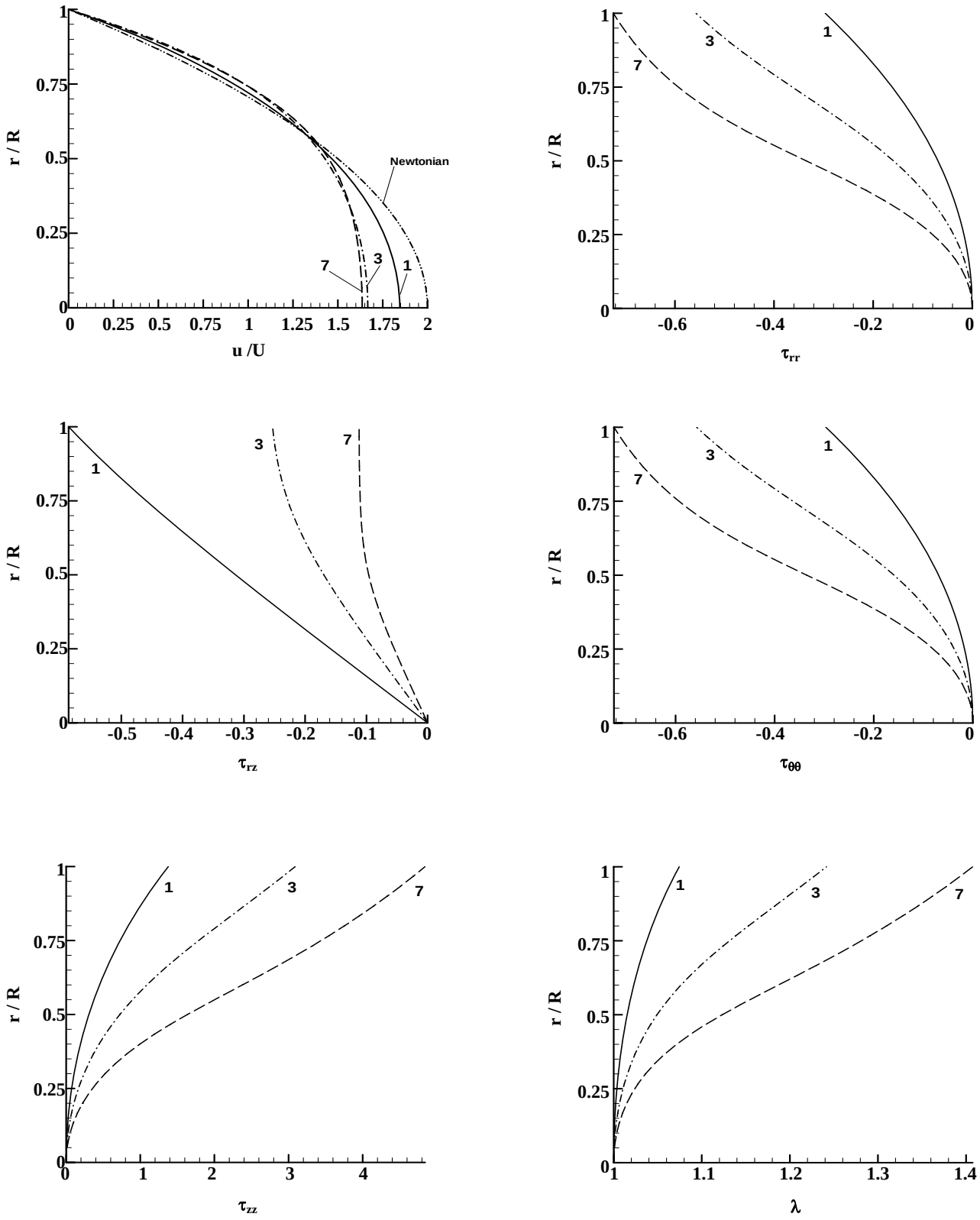

Fig. 3: Pipe flow, effect of We, Re=1, q =2, ε=1/3, β=1/9, α=0.15.

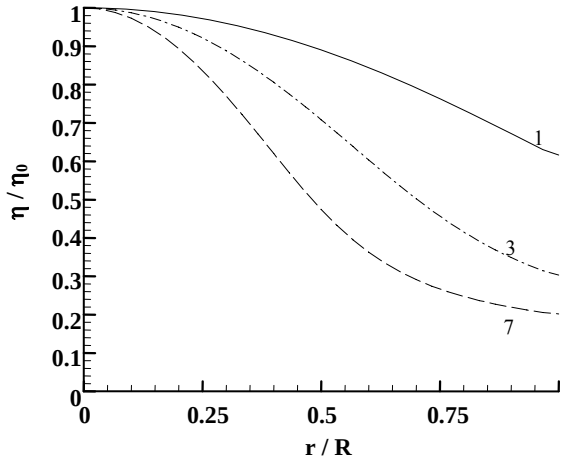

Fig. 4: Pipe flow, effect of We, Re=1, q =2, ε =1/3, β=1/9, α =0.15.

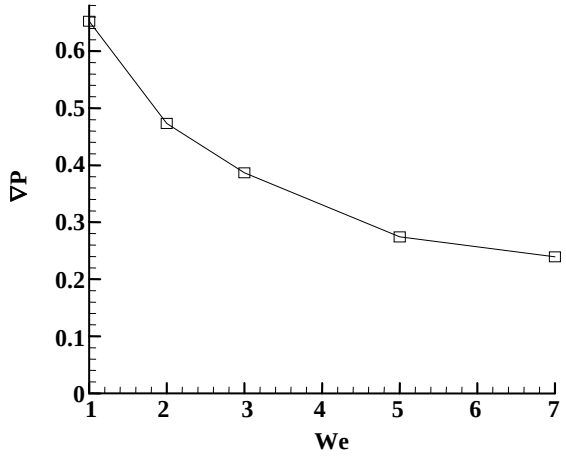

Fig. 5: Pipeflow, pressure gradient vs We, Re=1, q =2, ε =1/3, β=1/9, α =0.15.

Newtonian Fluid (GNF) model. "Power Law" model is used to represent the GNF. In power law model, the viscosity of polymeric liquids is defined as: $\eta = m\dot{\gamma}^{n-1}$; where η is viscosity, $\dot{\gamma}$ is shear rate; m and n are model parameters. Basically, the power law model does not include time constant (λ). Therefore, the limiting expression for the high shear rate which can be obtained from Carreau model, the m (consistency index) of the power law can be defined as: $m = \eta_0 \lambda^{n-1}$; where the exponent "n" in the power law model has the same meaning as the "n" in the Carreau model. (For more detail, see *Bird et al.* [16] chapter 4)

Therefore, one may check the accuracy of the present FV scheme by comparing it to the analytical solution of power law model for pipe flow problem. The following expressions have been obtained from the analytical solution for non-dimensional velocity and shear stress distribution of power law model in axisymmetry geometry (pipe) [16]:

$$\frac{u}{U} = \frac{(\frac{1}{n}+3)}{(\frac{1}{n}+1)} \left[(1-(r^*)^{\frac{1}{n}+1} \right] \qquad (21)$$

$$\tau_{rz} = We^{n-1} \left(\frac{1}{n}+3 \right)^n (r^*) \qquad (22)$$

$$r^* = (r/R)$$

$$\tau_{zz} = 0 \qquad \tau_{rr} = 0 \qquad (23)$$

In this study, the model parameters have been taken from the experimental data of viscosity and shear rate for LDPE (Low density Polyethylene), which is listed in table 3 [17]. By plotting $\ln(\eta)$ versus $\ln(\dot{\gamma})$, the power law parameters are obtained from the slope of the line in the linear region as follows:

m= 1.1219 E+4 Pa.s^n, n=0.51 and λ= 4.3 s^{-1}

Fig. 6 shows the results of XXP model and power law model. As it can be seen, the agreement between the results is good and the maximum error is less than 6% for both velocity and shear rate profiles (neglecting near the wall, for shear stress profile).

The XPP parameters are obtained from the 3rd mode of table 4 [9].

CONCLUSIONS

In this study we predicted the flow of branched polymers in pipe geometry with solving the governing equations for the extended pom-pom model, considering finite volume scheme.

At first we introduced the extended pom-pom model to eliminate and rectify perceived deficiencies of the original pom-pom model such as the lack of a second normal-stress difference and a discontinuity in the derivative of the extensional viscosity. Then we emphasized on the generation of steady-state profiles for velocity, stretch and extra-stress in pipe Poiseuille flow

Table 3: Steady shear rate and viscosity data for LDPE.

$\dot{\gamma}$ (s^{-1})	η (Pa.s)
0.01	2.31E+04
0.0215	2.22E+04
0.0464	2.01E+04
0.1	1.69E+04
0.215	1.44E+04
0.464	1.12E+04
1	8.19E+03

Table 4: XPP parameters data for LDPE (ν=2/q).

i	*Go* (pa)	λ_{ob}	$\varepsilon=\lambda_{os}/\lambda_{ob}$	*q*	α
1	7.2006E+4	3.8946E-3	1/7	1	0.3
2	1.5770E+4	5.1390E-2	1/5	1	0.3
3	3.3340E+3	4.3009E0	1/3	2	0.15
4	3.0080E+2	4.5911E+1	1.1	10	0.03

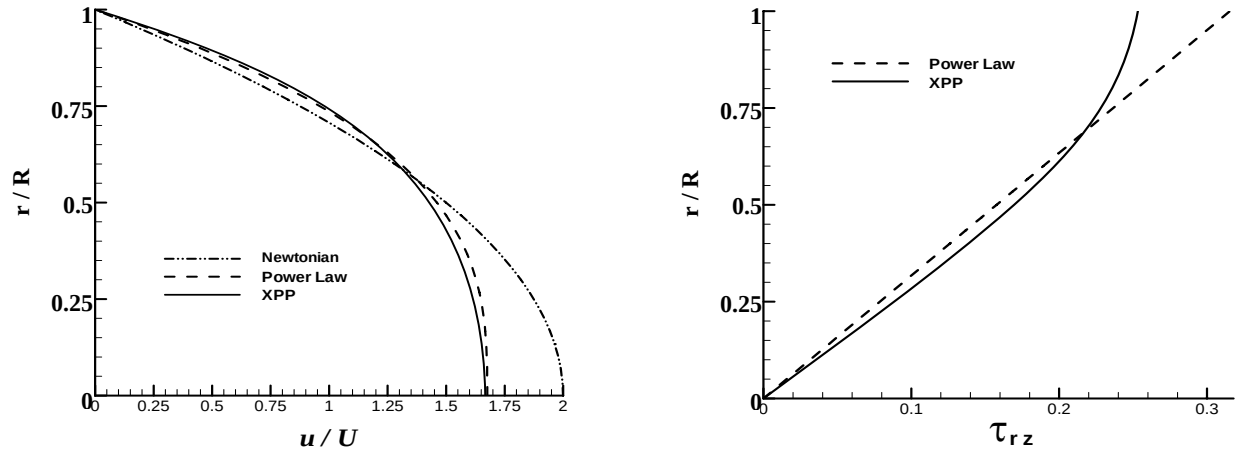

Fig. 6: Pipe flow, Comparison between XPP and Power law model at Re=1 and We=3. (for XPP model: q =2, ε=1/3, β=1/9, α=0.15 and for Power aw model: m=1.1219 E+4 , n=0.51)

that can be used as inflow conditions for complex planar flow problems.

Our finite volume method includes a scheme in which the solution of the conservation equations is decoupled from that solution of the constitutive equation at each iteration step. The diffusion terms in the momentum and constitutive equations are treated using an integration operator to discretise the governing equations in supposed control volume.

The results show when Weissenberg number increases the velocity profiles flatten in the center and shear extra-stress, τ_{rz}, gets smaller in absolute quantity. This effect is due to an increasing shear-thinning behaviour with increasing the Weissenberg number or elasticity parameter. So for identical pressure gradients, the XPP fluid can carry a larger flow rate than the Oldroyd-B or UCM fluids, especially for Weissenberg numbers larger than 2. Nevertheless, normal extra-stresses τ_{zz}, τ_{rr} and $\tau_{\theta\theta}$ get bigger (in absolute quantity) with increasing Weissenberg number and non-Newtonian fluid behaviour appears. The XPP model can predict extra-stress $\tau_{\theta\theta}$, while the other differential viscoelastic models cannot predict $\tau_{\theta\theta}$ in a two-dimensional fully developed pipe flow for viscoelastic fluid, this emphasizes that this model is a more potent model in simulating the viscoelastic fluid behaviour. Consequently, when Weissenberg number decreases the flow behaviour approaches to UCM or Newtonian fluid.

Finally, verification of the present model was made by comparing to the well-known Power Law model, which indicates a good agreement with numerical simulation confirming the ability of the XPP model to predict the flow of commercial polymer melts as illustrated.

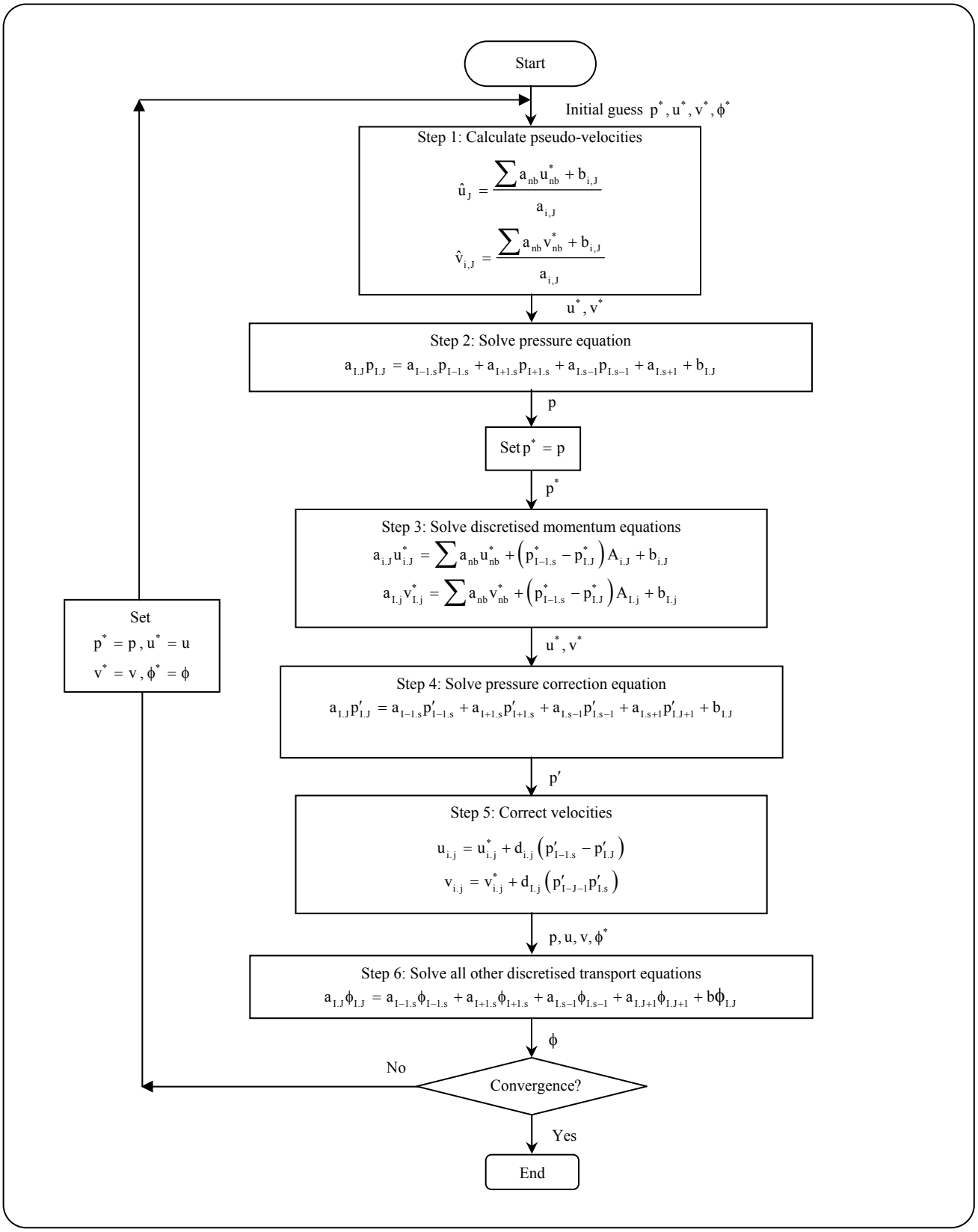

Fig. 7: SIMPLER algorithm flow diagram.

Appendix

Here, we use τ instead of ϕ, in the flow diagram, in Fig. 7.

Received : Sep. 16, 2009 ; Accepted : Apr. 19, 2010

REFERENCES

[1] McLeish T.C.B., Larson R.G., Molecular Constitutive Equations for a Class of Branched Polymers: the Pom-Pom Polymer, *J. Rheol.*, **42,** p. 81 (1998).

[2] Doi M., Edwards S.F., "The Theory of Polymer Dynamics", Oxford University Press, Oxford, (1986).

[3] Verbeeten W.M.H., Peters G.W.M., Baaijens F.T.P., Differential Constitutive Equations for Polymer Melts: the Extended Pom-Pom Model, *J. Rheol.*, **45** (4), p. 823 (2001).

[4] Van Os R.G.M., Phillips T.N., Spectral Element Methods for Transient Viscoelastic Flow Problems, *J. Comput. Phys.,* **201**, p. 286(2004).

[5] Van Os R.G.M., Phillips T.N., Efficient and Stable Spectral Element Methods for Predicting the Flow of an XPP Fluid Past a Cylinder, *J. Non-Newtonian Fluid Mech.*, **129**, p. 143 (2005).

[6] Van Os R.G.M., Phillips T.N., The Prediction of Complex Flows of Polymer Melts Using Spectral Elements, *J. Non-Newtonian Fluid Mech.*, **122**, p**.** 287 (2004).

[7] Blackwell R.J., McLeish T.C.B., Harlen O.G., Molecular Drag-Strain Coupling in Branched Polymer Melts, *J. Rheol.*, **44**, p. 121 (2000).

[8] Inkson N.J., Phillips T.N., van Os R.G.M., Numerical Simulation of Flow Past a Cylinder Using Models of XPP Type, *J. Non-Newtonian Fluid Mech.*, **156**, p. 7 (2009).

[9] Verbeeten W.M.H., Peters G.W.M., Baaijens F.T.P., Viscoelastic Analysis of Complex Melt Flows Using the Extended Pom-Pom Model, *J. Non-Newtonian Fluid Mech.*, **108,** p. 301 (2002).

[10] Phillips T.N., Williams A.J., Viscoelastic Flow Through a Planar Contraction Using a Semi -Lagrangian Finite Volume Method, *J. Non Newtonian Fluid Mech.,* **87,** p. 215 (1999).

[11] Aboubacar M., Phillips T.N., Tamaddon-Jahromi H.R., Snigerev B.A., Webster M.F., High-Order Finite Volume Methods for Viscoelastic Flow Problems, *J. Comput. Phys.,* **199,** p.16 (2004).

[12] Aboubacar M., Webster M.F., A Cell-Vertex Finite Volume/Element Method on Triangles for Abrupt Contraction Viscoelastic Flows, *J.Non-Newtonian Fluid Mech.*, **98**, p. 83 (2001).

[13] Patankar S.V., "Numerical Heat Transfer and Fluid Flow", McGraw-Hill, New York, (1980).

[14] Waters N.D., King M.J., "Unsteady Flow of an Elastico- Viscous Liquid", Acta Band 9, Heft 3 (1970).

[15] Bishko G.B., Harlen O.G., McLeish T.C.B., Nicholson T.M., Numerical Simulation of the Transient Flow of Branched Polymer Melts Through a Planar Contraction Using the 'Pom-Pom' Model, *J. Non-Newtonian Fluid Mech.*, **82**, p. 255 (1999).

[16] Byron Bird R., Armstrong R.C., Hassager O, "Dynamics of Polymeric Liquids", **1**, John-Wiley, New York, (1987).

[17] Baird D.G., "Polymer Processing: Principles and Design", Butterworth-Heinemann, (1995).